JOURNAL OF VIROLOGY, Dec. 1994, p. 8071–8081
0022-538X/94/$04.00+0

Vol. 68, No. 12

Two Open Reading Frames (ORF1 And ORF2) within the 2.0-Kilobase Latency-Associated Transcript of Herpes Simplex Virus Type 1 Are Not Essential for Reactivation from Latency

MOIN U. FAREED* AND JORDAN G. SPIVACK
The Wistar Institute, Philadelphia, Pennsylvania 19104

Received 18 July 1994/Accepted 13 September 1994

The herpes simplex virus type 1 (HSV-1) latency-associated transcripts (LATs) are dispensable for establishment and maintenance of latent infection. However, the LATs have been implicated in reactivation of the virus from its latent state. Since the reported LAT deletion and/or insertion variants that are reactivation impaired contain deletions in the putative LAT promoter, it is not known which LAT sequences are involved in reactivation. To examine the role of the 2.0-kb LAT in the process of reactivation and the functional importance of the putative open reading frames (ORF1 and ORF2) contained within the 2.0-kb LAT, we have constructed an HSV-1 variant that contains a precise deletion and insertion within the LAT-specific DNA sequences using site-directed mutagenesis. The HSV-1 variant FS1001K contains an 1,186-bp deletion starting precisely from the 5′ end of the 2.0-kb LAT and, for identification, a *Xba*I restriction endonuclease site insertion. The FS1001K genome contains no other deletions and/or insertions as analyzed by a variety of restriction endonucleases. The deletion in FS1001K removes the entire 556-bp intron within the 2.0-kb LAT, the first 229 nucleotides of ORF1, and the first 159 nucleotides of ORF2 without having an affect on the RL2 (ICP0) gene. Explant cocultivation reactivation assays indicated that this deletion had a minimal effect on reactivation of the variant FS1001K compared with the parental wild-type virus using a mouse eye model. As expected, Northern (RNA) blot analyses have shown that the variant virus (FS1001K) does not produce the 2.0-kb LAT or the 1.45- to 1.5-kb LAT either in vitro or in vivo; however, FS1001K produces an intact RL2 transcript in tissue culture. These data suggest that the 2.0-kb LAT putative ORF1 and ORF2 (or the first 1,186 bp of the 2.0-kb LAT) are dispensable for explant reactivation of latent HSV-1.

A unique and biologically important feature of herpesviruses is their ability to establish and maintain latent infections within their natural hosts. The virus may remain in a noninfectious latent state for years and then reactivate to produce viral shedding, infection of naive individuals, and sometimes recurrent disease. Following primary infection, some herpesviruses, an example of which is herpes simplex virus type 1 (HSV-1), establish latency in the sensory ganglion innervating the dermatome, while others, an example of which is Epstein-Barr virus, are lymphotropic.

During HSV-1 latency, viral DNA has been detected (48, 49) and probably exists as a circular or concatemeric form in an episomal state (14, 19, 41, 49). Latent viral gene expression and transcription are limited to a single transcription unit, which produces the latency-associated transcripts (LATs) (12, 50, 56, 61). Three LATs of 2.0, 1.5, and 1.45 kb have been detected by Northern (RNA) blot analysis, of which the smaller transcripts are spliced from the largest (56, 59, 65, 66). The 2.0-kb transcript is stable, poorly polyadenylated, and localized within the ganglionic cell nuclei (56, 64, 65). The last 723 bases of the stable LAT are complementary to and overlap with the HSV-1 RL2 gene (IE-1, IE110, or ICP0 [56, 61, 64, 66]). Using in situ hybridization, it has been shown that possibly a larger (8- to 10-kb) region is transcriptionally active during latency (13, 42, 72). This large hypothetical RNA, which is termed minor LAT (m-LAT), is presumed to be unstable and processed to form the smaller, more stable LATs (for a review, see reference 24). The 2.0-kb LAT may be an intron (22) containing another intron (59) and might therefore be referred as a twintron (9). The 2.0-kb LAT also contains two putative open reading frames (ORF1 and ORF2) (Fig. 1) (59, 66). However, expression of these or any other LAT-encoded products in vivo remains to be demonstrated.

The use of deletion and/or insertion variants in functional characterization of HSV-1 genes is well documented (see, for example, references 1, 8, 36, 45, and 47). Similarly, LAT deletion and/or insertion variants have also proved useful in functional analysis of these transcripts (3, 4, 17, 23, 27–29, 32, 38, 43, 53, 54, 60, 63). However, most of the variants used in these studies involve either the putative LAT promoter region alone (17, 27, 29, 53) or in conjunction with the 2.0-kb LAT sequences (3, 32, 43, 53, 60, 63). These studies have demonstrated that detectable amounts of LATs (using Northern blot analysis and in situ hybridization techniques) are not required for the establishment or maintenance of the latent infection but may play a role in efficient (wild-type [WT] levels) reactivation from latency. However, because these HSV-1 variants have promoter mutations, they have not provided information concerning which region(s) of the LAT transcription unit is involved in reactivation. Furthermore, the use of HSV-1 variants, such as TB1 (4), RH142 (28), and RP1 (23), has indicated that some deletions and/or insertions within the 2.0-kb LAT or ORF1 do not affect the process of reactivation.

None of the variants reported thus far contain a deletion that starts precisely at the 5′ end of the 2.0-kb LAT or a deletion and/or insertion disrupting the putative ORF2 of

* Corresponding author. Mailing address: The Wistar Institute, 36th Street at Spruce, Philadelphia, PA 19104. Phone: (215) 898 0127. Fax: (215) 898 3868.

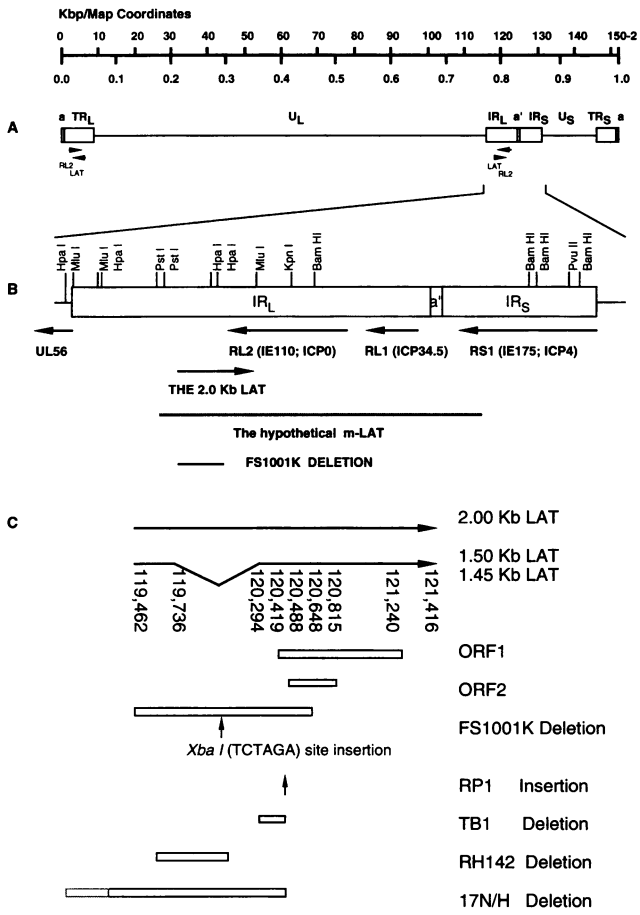

FIG. 1. Map of the deletion and insertion in the variant FS1001K. (A) Structure of the HSV-1 genome in the prototype orientation. The long unique (U_L) and short unique (U_S) regions, their TR_L and TR_S and IR_L and IR_S elements, and the "a" sequence are indicated. The position and direction of RL2 (ICP0) and the 2.0-kb LAT transcripts are shown by arrowheads below the TR_L and IR_L. (B) Expanded joint region (the repeat elements, IR_L, the inverted "a" sequence, and IR_S are indicated by open boxes, while the unique sequences are indicated by solid lines) showing the locations of HSV-1 genes RS1, RL1, and RL2, the 2.0-kb LAT, the m-LAT, and the UL56 gene. The commonly used restriction endonuclease sites are shown above the expanded region. (C) The 2.0-, 1.5-, and 1.45-kb LATs, putative ORFs (ORF1 and ORF2) within these LATs, map of the 1,186-bp deletion in the HSV-1 strain KOS variant FS1001K starting precisely from the 5′ end of the 2.0-kb LAT (nt 6910 and 119,462), and an *Xba*I restriction endonuclease site insertion. The nucleotide numbers represent the numbering system of the HSV-1 DNA sequence described by McGeoch et al. (39). Aproximate boundries of deletions and/or insertions in HSV-1 variants 17N/H (3), RH142 (28), TB1 (4 [the variant TB1 actually contains a 4.1-kb deletion in IR_L because of its HFEM background, therefore, the constructed deletion and insertion are in the TR_L only]), and RP1 (23) are also shown in panel C in comparison with the deletion and insertion in FS1001K.

the 2.0-kb LAT. Thus, the role of the 2.0-kb LAT in the reactivation process of HSV-1 is still poorly understood. In order to functionally characterize the 2.0-kb LAT as well as ORF2, an HSV-1 LAT-negative variant, FS1001K, containing an 1,186-bp deletion starting precisely from the 5′ end of the 2.0-kb LAT and insertion of an *Xba*I restriction endonuclease site was generated. FS1001K deletes the entire intron within the 2.0-kb LAT (59), the first 229 nucleotides (nt) of ORF1, and the first 159 nt of the LAT ORF2. The deletion does not affect the LAT promoter, the RL2 transcript, or RL2 regulatory sequences. The data indicate that neither ORF1 nor ORF2 within the 2.0-kb LAT, which are also contained within the 1.45- to 1.5-kb LAT, is required for establishment of HSV-1 latency or reactivation from explanted trigeminal ganglia (TG). Furthermore, the deletion in FS1001K abolishes the putative splice donor signal at the 5′ end of the 2.0-kb LAT. Therefore, the proposed 6.0-kb spliced RNA, which would result after removal of the 2.0-kb LAT from an 8.0-kb m-LAT, cannot be synthesized during latent infection of FS1001K. These data indicate that neither the 2.0-kb LAT, nor the 1.45- and 1.5-kb spliced LATs, nor the hypothetical 6.0-kb spliced RNA is required for efficient reactivation of latent HSV-1.

MATERIALS AND METHODS

Cells. Baby hamster kidney 21 clone 13 (BHK21/C13) cells (37) were grown in Eagle's medium containing twice the normal concentration of vitamins and amino acids, 10% (vol/vol) tryptose phosphate broth, and 10% (vol/vol) calf serum (ETC10) at 37°C with 5% CO_2.

Viruses. HSV-1 Glasgow strain 17^+ (7) and HSV-1 strain KOS (obtained from Nigel W. Fraser, The Wistar Institute) were the parental WT viruses used in most experiments. The variant FS1001K was generated in a strain KOS (M) background with the exception of a 2,659-bp restriction endonuclease fragment (see below). High-titer virus stocks were propagated in BHK21/C13 cells. Confluent cell monolayers in 175-cm^2 tissue culture flasks were infected with HSV-1 at a multiplicity of infection (MOI) of 0.003 PFU per cell in 20 ml of ETC10. The flasks were incubated at 31°C for 3 to 5 days or until the appearance of extensive cytopathic effect (CPE). Virus was concentrated from the medium as previously described (12, 13, 20) and titrated on BHK21/C13 cell monolayers. The plaques were fixed and stained with 1% methylene blue or Giemsa stain and were counted.

Preparation of virion DNA. Viral DNA was obtained as previously described (6, 68).

Plasmids. The phagemid vectors pGEM3Zf(−) and pGEM3Zf(+) (Promega) were used to clone HSV-1 strain 17^+ DNA containing the 2.0-kb LAT. The plasmids pMF201 and pMF202 were constructed by cloning the *Pst*I-*Kpn*I (nt 118866 to 122711) fragment into the multiple cloning regions of pGEM3Zf(−) and pGEM3Zf(+), respectively (Fig. 2). The nucleotide numbers given represent the first base of the respective restriction endonuclease cleavage site of HSV-1 strain 17^+ DNA, as described by McGeoch et al. (39).

Preparation of plasmid DNA. Plasmid DNA was prepared according to the method described by Birnboim and Doly (2) and was further purified by using the Prep-A-Gene purification kit (Bio-Rad).

Site-directed mutagenesis. The mutagenic oligonucleotides (Table 1) were synthesized at the Oligonucleotide Synthesis Laboratory of The Wistar Institute. Site-directed mutagenesis was carried out essentially as described by Kunkel (30) and Kunkel et al. (31). Briefly, *Escherichia coli* BW313 (30, 40) or CJ236 (purchased from Bio-Rad) was transformed with the parental plasmid, and uracil-rich single-stranded DNA was prepared by infecting bacterial cultures grown in a medium containing 0.25 mg of uridine per ml with helper phage M13 KO7 or M13 R408 at an MOI of approximately 20. Single-stranded DNA precipitation was carried out by the addition of a 0.25 volume of 3.5 M ammonium acetate–20% (wt/vol) polyethylene glycol 8000 solution. DNA was extracted with phenol-chloroform and reprecipitated with 3 M sodium ace-

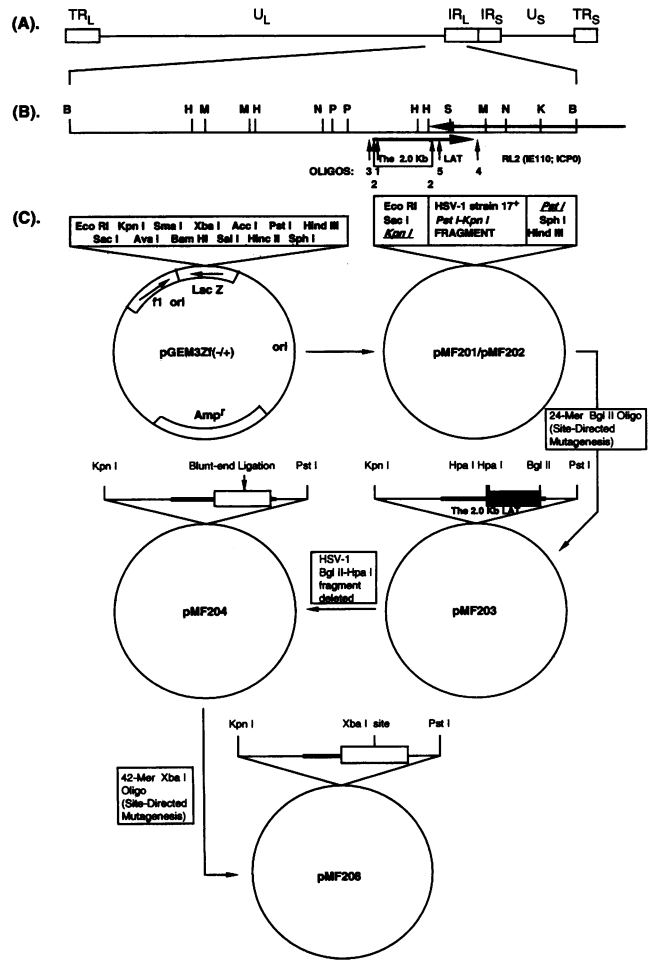

FIG. 2. Construction of wild-type and mutant plasmids. (A) HSV-1 genome structure in the prototype orientation. (B) Expansion of the HSV-1 strain 17^+ *Bam*HI b (nt 113,322 to 123,459) fragment showing *Bam*HI (B), *Hpa*I (H), *Kpn*I (K), *Mlu*I (M), *Not*I (N), *Pst*I (P), and *Sal*I (S) restriction endonuclease sites (above the line). The locations of oligonucleotides used in site-directed mutagenesis (nos. 1 and 2) and DNA sequence determinations (nos. 3, 4, and 5) are also shown below the line (see Table 1). The locations of the 2.0-kb LAT and RL2 (IE110 or ICP0) transcripts are indicated by thick arrows. The arrowheads indicate the directions of transcription. (C) The HSV-1 *Pst*I-*Kpn*I fragment containing the 2.0-kb LAT was cloned into the respective restriction endonuclease sites within the multiple cloning site region of phagemids pGEM3zf(−) and pGEM3zf(+) to generate plasmids pMF201 and pMF202, respectively. The plasmid pMF201 was used in site-directed mutagenesis along with the 24-mer *Bgl*II oligonucleotide (no. 1 in Table 1) to create a *Bgl*II site 10 bases downstream of the 5′ end of the 2.0-kb LAT. The resultant plasmid was designated pMF203. The *Bgl*II-*Hpa*I fragment (996 bp [filled box]) was deleted (empty box) from pMF203 to generate pMF204. A second round of site-directed mutagenesis was carried out using the plasmid pMF204 and the 42-mer *Xba*I oligonucleotide (no. 2 in Table 1), and a plasmid (pMF208) containing a 1,186-bp deletion (empty box) starting precisely from the 5′ end of the 2.0-kb LAT (nt 119,462) and an insertion of 6 bp (*Xba*I site [TCTAGA]) was isolated.

tate or 5 M NaCl and ethanol. The appropriate mutagenic oligonucleotide was 5′ phosphorylated and annealed to the complementary uracil-rich single-stranded DNA at a molar ratio of 20:1. The primer extension reaction was carried out at 15°C for 16 h in the presence of 1 mM ATP, 100 μM each deoxynucleoside triphosphates, 100 μg of gene 32 protein per ml, 2 U of the Klenow fragment of DNA polymerase I, and 4 U of T4 DNA ligase. The reaction mixture was transformed into *E. coli* DH5α cells (GIBCO BRL) to ampicillin resistance, and mutant plasmids were identified by restriction endonuclease digestion analysis.

DNA sequence determinations. DNA sequences of mutant plasmids were determined using double-stranded DNA templates and the Sequenase version 2.0 DNA sequencing kit (U.S. Biochemical) as described by Spivack et al. (59).

Construction of the variant virus. BHK21/C13 cell monolayers (4×10^6 cells) were transfected with DNA by the calcium phosphate procedure described by Stow and Wilkie (62). HSV DNA (1 to 2 μg) was cotransfected with 5-, 10-, and 20-fold molar excesses of linearized mutant plasmid in the presence of carrier calf thymus DNA to a total of 5 μg of DNA per transfection. The transfection plates were incubated at 37°C in Eagle's medium containing 5% (vol/vol) calf serum until the appearance of widespread CPE. The cells were then scraped into the medium and sonicated, and virus was titrated. Individual plaques obtained from the titrated transfection plate stocks were isolated and grown in 24-well-plate (Falcon) stocks, and their genome structures were determined by restriction endonuclease digestion analysis. After the desired variant virus was found, it was plaque purified an additional three times prior to the production of a high-titer virus stock.

Restriction endonuclease analysis of virus genomes. Restriction endonuclease analysis was carried out by a modification of the method described by Lonsdale (33). Cells were infected in the presence of $^{32}P_i$ in phosphate-free Eagle's medium containing 1% (vol/vol) calf serum and were incubated at 31°C for at least 48 h. ^{32}P-labelled virus DNA was extracted with sodium dodecyl sulfate (SDS) and phenol and ethanol precipitated. The DNA was subjected to digestion with appropriate restriction endonucleases under the manufacturer's recommended conditions and was analyzed by electrophoresis on agarose gels with the appropriate concentrations (0.5 to 1.2%) in TBE buffer (89 mM Tris, 89 mM boric acid, 2 mM sodium EDTA). The gels were air dried and exposed to Kodak X-Omat film for 24 to 72 h.

Infection of mice. BALB/c mice (Jackson Laboratory, Bar Harbor, Maine) that were 4 to 6 weeks old were anesthetized with Metofane (Pitman-Moore, Inc., Mundelein, Ill.), their corneas were scarified, and 2×10^6 PFU of HSV-1 strain KOS or the variant FS1001K was added per eye. The viruses were diluted in ETC10, and 5 μl of the diluted virus was used for each eye.

Explant cocultivation reactivation assay. At a minimum of 28 days postinfection, latently infected mice were scarified by cervical dislocation, and their eyes and TG were removed aseptically and processed for RNA isolation or incubated on BHK21/C13 cell monolayers grown in 6-well tissue culture plates (Falcon). The plates were incubated at 37°C, and the tissues were transferred onto fresh cell monolayers every 3 to 4 days for a total of 35 days. Once viral CPE was observed, reactivated virus was harvested and stored at −70°C for restriction endonuclease analysis.

Extraction of RNA and Northern blot analysis. Total RNA was prepared as previously described (56, 57). Briefly, pooled TG from five latently infected mice were homogenized in 4 M guanidium thiocyanate–0.5% sodium-*N*-lauroylsarcosine–100 mM β-mercaptoethanol–25 mM sodium citrate–0.1% Antifoam A (Sigma) for 20 s using an electric cell disrupter (Tekmar, Cincinnati, Ohio). Tissue culture cells were harvested in phosphate-buffered saline, pelleted by low-speed centrifugation for 10 min at 4°C, and homogenized in gua-

TABLE 1. Synthetic oligonucleotides used in site-directed mutagenesis and DNA sequence determinations[a]

Oligonucleotide	Sequence
*Bgl*II 24-mer (no. 1)[b]	(119462–119485)[c]
WT DNA sequence (strain 17$^+$):	5′-GTAGGTTAGA**C**A**C**CTGCTTCTCCC-3′
Mutant DNA sequence (FS1001K)	5′-GTAGGTTAGA**GATCT**GCTTCTCCC-3′
	*Bgl*II site
*Xba*I 42-mer (no. 2)[d]	(119444–119461–*Xba*I–120648–120665)[c]
WT DNA sequence (strain 17$^+$)	5′-AAGACGCCGCGTTTCCAG-------TACATCCAACACAGACAG-3′
	(119462–119464)[e] GTA....CGA (120645–120647)[e]
Mutant DNA sequence (FS1001K)	5′-AAGACGCCGCGTTTCCAG**TCTAGA**TACATCCAACACAGACAG-3′
	*Xba*I site
PF 5′ LAT 22-mer (no. 3)[f]	(119376–119397)[c]
	5′-AGTACCCTCCTCCCTCCCTTCC-3′
PR 3′ LAT 22-mer (no. 4)[f,g]	(121476–121497)[c]
	5′ACCCCCGCGGGGGCCGCCTCTT-3′
PR 3′ LAT RL.2 22-mer (no. 5)[g]	(120697–120718)[c]
	5′-AGGGGATTTTTGCTGTCTGTTG-3′

[a] For locations of these oligonucleotides, see Fig. 2B. Oligonucleotides 1 and 2 were used in site-directed mutagenesis, whereas oligonucleotides 3, 4, and 5 were used in DNA sequence determinations. PF, forward primer; PR, reverse primer.

[b] The *Bgl*II oligonucleotide was used to create a *Bgl*II site 10 bases downstream of the 5′ end of the 2.0-kb LAT by two single-base alterations (indicated with bold and underlined letters).

[c] The nucleotide numbers in parentheses above the sequences are those of HSV-1 strain 17$^+$ DNA (39).

[d] The *Xba*I oligonucleotide was used to generate a 1,186-bp deletion starting precisely from the 5′ end of the 2.0-kb LAT and, for identification, to insert a *Xba*I site.

[e] The 1,186-bp deletion generated in FS1001K includes these nucleotides of 17$^+$ DNA (39).

[f] These oligonucleotides were used in sequence determination of plasmid pMF203 (see Fig. 2C).

[g] These oligonucleotides were used as primer to determine the DNA sequence of pasmid pMF208 (see Fig. 2C).

nidium solution as described for TG. Infected BHK21/C13 cells were harvested at various times (8 to 16 h) postinfection to get better expression of RL2 mRNA compared with the 2.0-kb LAT (56–58). RNA was pelleted through a CsCl cushion (40,000 rpm in a Beckman SW55 rotor for 22 h at 18°C). The pellets were resuspended in water and ethanol precipitated. Glyoxal-treated RNA (5 to 10 μg per lane) was run on a 1.2% agarose gel, and the gel was stained with acridine orange to confirm that the amounts of RNA were equal in all gel tracks and was capillary blotted to GeneScreen Plus (Dupont). RNA markers were purchased from Bethesda Research Laboratories, Inc. The GeneScreen Plus filters were air dried, and glyoxylation was reversed as previously described (56, 57). ^{32}P-labelled, heat-denatured, and nick-translated DNA probes were hybridized to Northern blots overnight (56, 57). Filters were washed in decreasing concentrations of SSC (1× SSC is 0.15 M NaCl plus 0.015 M sodium citrate, pH 7.0) from 1.0× to 0.1× with 1% SDS at 65°C (twice for 30 min per wash), air dried, and exposed to Kodak X-Omat films with intensifying screens (Dupont) at −70°C.

Preparation of ^{32}P-labelled probes. The HSV-1 strain F *Pst*I-*Mlu*I (nt 118,866 to 121,651) and strain 17$^+$ *Pst*I-*Kpn*I (nt 118,866 to 122,711) DNA fragments were gel purified (see Fig. 2B for the positions of these fragments), nick translated to a specific activity of 1×10^8 to 5×10^8 cpm/μg of DNA (51), and used as the dual LAT-RL2 probes. The labelled probes were separated from unincorporated nucleotides by passage through Quick Spin Sephadex columns (Boehringer-Mannheim).

RESULTS

Construction of mutant plasmids. Initially, the plasmid pMF201 was used with the 42-mer mutagenic oligonucleotide (Table 1, no. 2) in site-directed mutagenesis (30, 31) to create a 1,186-bp deletion. However, attempts to isolate the desired mutant plasmid failed, possibly because of a very large looped-out region and the high GC content of HSV-1 repeat elements (39, 51). Moreover, the efficiency of oligonucleotide-mediated mutagenesis decreases as the size of the mutation to be constructed increases (51). Therefore, it was decided to carry out several rounds of site-directed mutagenesis to generate the desired mutant plasmid. The first round of site-directed mutagenesis involved the plasmid pMF201 and the 24-mer oligonucleotide (Table 1, no. 1; Fig. 2B). Following in vitro mutagenesis reactions and transformations, plasmid DNAs from the resultant bacterial colonies were analyzed with the *Bgl*II restriction endonuclease, mutant plasmids containing a unique *Bgl*II site near the 5′ end of the 2.0-kb LAT were isolated (data not shown), and their DNA sequences were determined (using oligonucleotides 3 and 4 [Table 1]). One of these plasmids, pMF203 (Fig. 2C), was completely digested with the *Bgl*II (nt 119,472) and *Hpa*I (nt 120,300 and 120,468) restriction endonucleases and gel purified, and the fragment (lacking the 996-bp *Bgl*II-*Hpa*I fragment) was filled in with the Klenow fragment of DNA polymerase I (51) and self-ligated to generate plasmid pMF204 (Fig. 2C). A second round of oligonucleotide-mediated mutagenesis (30, 31) was then carried out using the plasmid pMF204 with the 42-mer oligonucleotide (Table 1; Fig. 2B). Following transformation of in vitro mutagenized pMF204 DNA, bacterial colonies were screened and mutant plasmids lacking an additional 190 bp (a total of 1,186 bp) of the 2.0-kb LAT-specific sequences were isolated. The precise nature of the deletion was confirmed by restriction endonuclease analysis and DNA sequencing (the oligonucleotides PF 5′ LAT and PR 3′ LAT RL2 [Table 1; Fig. 2B] were used for sequence determinations; data not shown). A mutant plasmid, designated pMF208 (Fig. 2C), was used in marker transfer experiments (see below).

Isolation and analysis of the variant FS1001K. The 1,186-bp deletion created in plasmid pMF208 was marker transferred into HSV-1 strain KOS (M). Progeny virus was harvested and

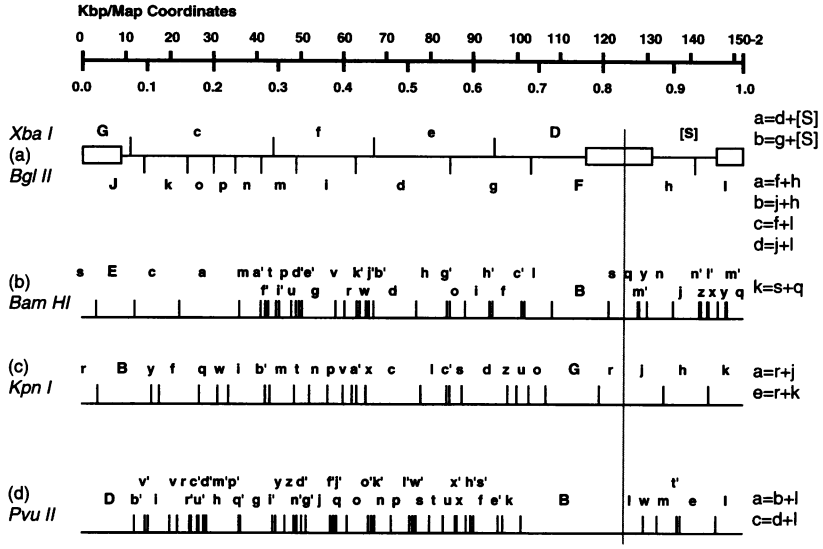

FIG. 3. Restriction endonuclease maps of the HSV-1 strain 17$^+$ genome. (a) The *Xba*I (above the line) and *Bgl*II (below the line) maps for the DNA of HSV-1 strain 17$^+$ (69, 70). The two *Bgl*II sites between the *Bgl*II fragments k and o (231 bp apart) and o and p (426 bp apart) are each shown as a single site. The *Bam*HI (b), *Kpn*I (c), and *Pvu*II (d) restriction endonuclease maps of HSV-1 Glasgow strain 17$^+$ (10) are shown. The positions of restriction endonuclease sites are approximate in this figure. The restriction endonuclease fragments affected by the deletion in the HSV-1 variant FS1001K are highlighted by capital letters. The joint fragments seen in restriction endonuclease DNA profiles of HSV-1 strain 17$^+$ are indicated on the right-hand side of the maps.

titrated, and 200 single, well-separated plaques were picked and grown in 24-well tissue culture plates to generate virus stocks. These plaque isolates were then examined by restriction endonuclease analysis of their ^{32}P-labelled DNAs (33). Since a *Xba*I restriction endonuclease site was inserted in the mutant plasmid pMF208 (Table 1; Fig. 2C), these plaque isolates were initially screened by *Xba*I restriction endonuclease digestion analysis of their DNAs. The *Xba*I profile of one of these differed from that of strain KOS DNA (Fig. 3a and 4, lane 2). The WT (strain KOS) viral genome contains four *Xba*I sites (55). Generation of an extra *Xba*I site within the long repeat (R_L) segment of the viral genome would cleave the *Xba*I g fragment (M_r, 7.10 × 10^6) into two smaller g′ fragments as well as the *Xba*I d (M_r, 18.20 × 10^6) into two d′ fragments. Taking into consideration a deletion with an approximate M_r of 0.78 × 10^6 (1,186 bp), the novel d′ fragments would have M_r values of 14.20 × 10^6 and 3.22 × 10^6, respectively. Similarly, the novel g′ fragments would have M_rs of 3.87 × 10^6 and 2.45 × 10^6, respectively. In addition, the joint fragments a and b would be reduced to a′ and b′, respectively (Table 2). The *Xba*I profile of the variant FS1001K is shown in Fig. 4, lane 2. It can be seen that the novel d′ bands run below the *Xba*I f and g bands, respectively, whereas the novel g′ bands migrate much lower, as expected (the sizes of the *Xba*I g′ bands and smaller d′ bands can be compared with the *Bgl*II m, n, and p bands in Table 2 and Fig. 4, lane 4). The reduced joint fragments, a′ and b′, are not resolved in the *Xba*I profile of FS1001K (Fig. 4, lane 2) because of their comigration with the *Xba*I c and e bands (Table 2). Moreover, the *Xba*I restriction endonuclease often gives partial digests (~5 to 10%) of HSV DNA in our hands. Therefore, a *Bgl*II-*Xba*I double digest of strain 17$^+$, strain KOS, and the variant FS1001K DNAs was carried out. HSV-1 strain 17$^+$ DNA was included in these analyses because its complete DNA sequence has already been published (39), and detailed maps for most of the commonly used restriction endonucleases are available (10, 69, 70).

The HSV-1 strain 17$^+$ genome contains 12 *Bgl*II and 4 *Xba*I sites (Fig. 3a). The *Xba*I sites are located at 0.07, 0.29, 0.45, and 0.63 map coordinates (mc) and are contained within the *Bgl*II j, m, d, and g fragments, respectively (Fig. 3a). Thus, the 0.07-mc *Xba*I site cleaves the *Bgl*II j fragment into two smaller j′ fragments (Table 2). In addition, the j fragment-containing joints b and e are reduced and comigrate with c (b′) and d′ (e′), respectively (Table 2). The *Bgl*II m fragment is cleaved by the 0.29-mc *Xba*I site into two smaller m′ bands, the *Xba*I site at 0.45 mc cuts the *Bgl*II d fragment into two smaller d′ bands, and the *Bgl*II g fragment is cleaved by the *Xba*I site at 0.63 mc into two g′ bands (Table 2). Because of the presence of an additional *Xba*I site and an 1,186-bp deletion (in both the terminal and the internal R_Ls [TR_L and IR_L, respectively]) within the genome of the variant (FS1001K), the *Bgl*II j′ (M_r, 7.10 × 10^6) band would be further cleaved into two smaller j″ bands (M_rs, 3.82 × 10^6 and 2.50 × 10^6), which would migrate with the *Bgl*II n and below the j′ (M_r 2.60 × 10^6) bands, respectively. Furthermore, the j′ fragment-containing joint fragments b′ and e′ (see above) would be further reduced into b″ and e″ bands, respectively (Table 2). In addition, the *Bgl*II f fragment would be cleaved into two smaller f′ bands, which would migrate below the c′ and n bands, respectively. The f fragment-containing joints a (a′) and c (c′) would also be reduced and run with the b″ and below the e″ bands, respectively (see Table 2 for M_rs of the *Bgl*II bands). The *Bgl*II profile of HSV-1 strain 17$^+$ DNA can be seen in Fig.4, lane 4. The *Bgl*II-*Xba*I profiles of strain 17$^+$, variant FS1001K, and strain KOS DNAs are shown in Fig. 4, lanes 5, 6, and 7. It can be seen that the *Bgl*II b″, a′, e″, c′, f′, and j″ bands (labelled on the right-hand side of lane 6 in Fig. 4) migrate at their expected positions (Table 2; compare lane 6 with lanes 5 and 7 in Fig. 4). Thus, the variant (FS1001K) contains the expected deletion and additional *Xba*I sites. Moreover, the *Bgl*II-*Xba*I double digest has resolved the high-molecular-weight bands (as seen in *Xba*I digest [Fig. 4, lane 2]), and no contaminating WT band could be detected in the FS1001K DNA profile (Fig. 4, lane 6).

To find out whether the genome of FS1001K contains any

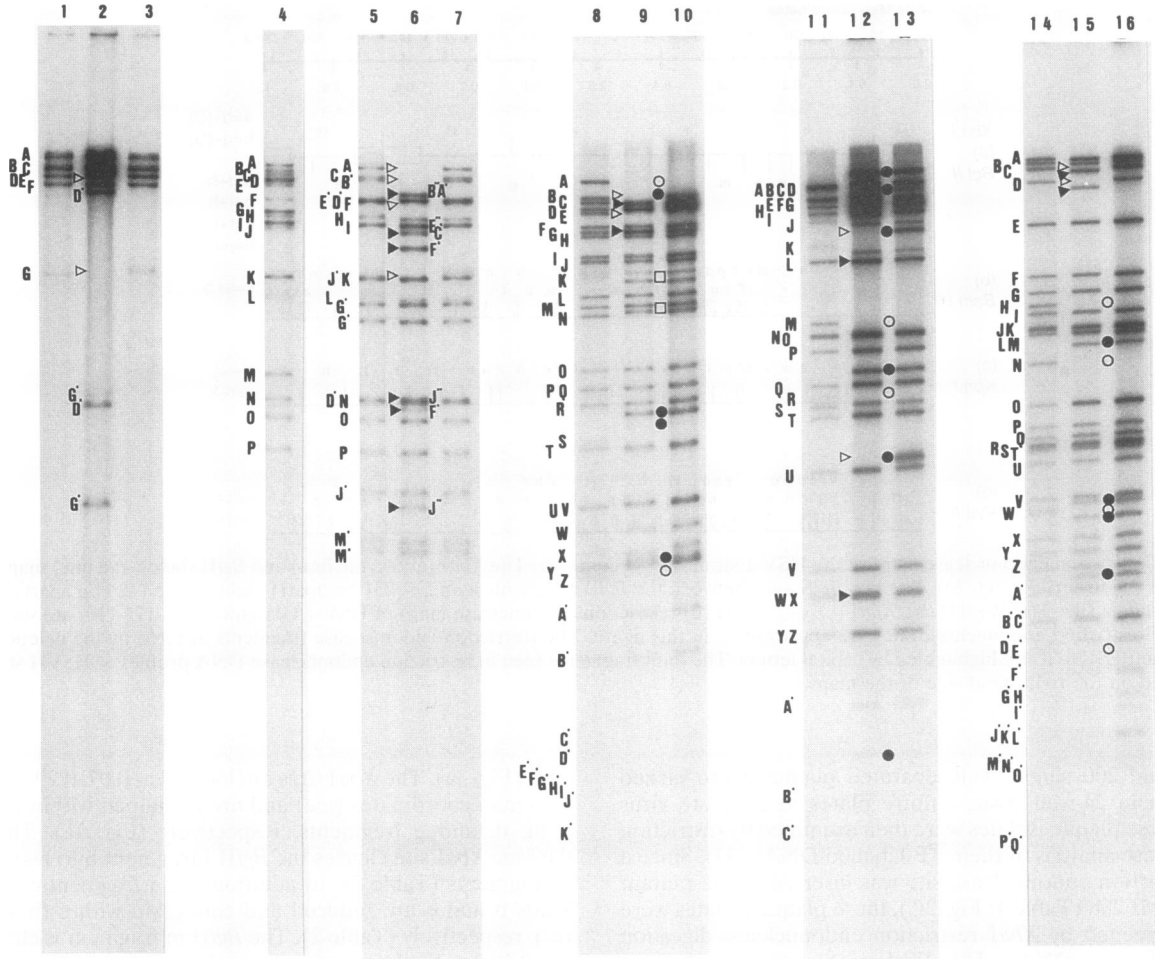

FIG. 4. Restriction endonuclease profiles of HSV-1 strain 17^+, strain KOS, and the variant FS1001K DNAs. The *Xba*I (lanes 1 to 3), *Bgl*II (lane 4), *Bgl*II-*Xba*I (lanes 5 to 7), *Bam*HI (lanes 8 to 10), *Kpn*I (Lanes 11 to 13), and *Pvu*II (lanes 14 to 16) restriction endonuclease profiles of HSV-1 strain 17^+ (lanes 1, 4, 5, 8, 11, and 14), strain KOS (lanes 3, 7, 10, 13, and 16), and the variant FS1001K (lanes 2, 6, 9, 12, and 15) DNAs ^{32}P-labelled in vivo (0.5 and 0.8% agarose gels) are shown. The strain 17^+ restriction endonuclease bands are labelled on the left-hand side of lanes 1, 4, 5, 8, 11, and 14. The missing bands in FS1001K DNA profiles are indicated by open triangles, and the novel bands are indicated by filled triangles. In lane 2, the *Xba*I novel bands are labelled on the left-hand side, whereas in lane 6, the novel *Bgl*II bands are labelled on the right-hand side. In strain KOS DNA profiles, the missing bands (compared with strain 17^+ DNA profiles) are indicated by open circles, whereas the additional bands are indicated by filled circles. A slight difference(s) in the mobility of the respective restriction endonuclease band(s) in the strain KOS DNA profile compared with that of strain 17^+ is indicated by an open square.

other deletion and/or insertion, it was necessary to analyze it with restriction endonucleases which cleave HSV-1 DNA more frequently than *Xba*I. Such analyses allow the identification of deletions or insertions greater than ~150 bp (20). Therefore, HSV-1 strain 17^+, strain KOS, and FS1001K DNAs were analyzed with the *Bam*HI, *Bgl*II, *Bgl*II-*Xba*I, *Kpn*I, *Pvu*II (Fig. 4), *Eco*RI, *Hin*dIII, *Bgl*II-*Hin*dIII, and *Hpa*I (data not shown) restriction endonucleases. No prominent alterations (the fragments containing the repeat elements [joints or ends] normally show variations among plaque isolates of a single WT strain [11, 20, 34, 35]) were found in these analyses (Fig. 3 and 4; data not shown). The published restriction endonuclease mapping data of HSV-1 strain KOS consists of *Bgl*II, *Eco*RI, *Hin*dIII, *Hpa*I, and *Xba*I (26, 44, 52, 55). Therefore, for the restriction endonucleases *Bam*HI, *Kpn*I, and *Pvu*II, we have used the HSV-1 strain 17^+ mapping data (Fig. 3) (10) and compared the DNA profiles of strain 17^+, strain KOS, and the variant FS1001K (Fig. 4). The structure of the variant (FS1001K) is shown in Fig. 1B and C, along with the arrangement of HSV-1 genes surrounding the LAT-specific sequences and, deletions and/or insertions in HSV-1 variants 17N/H (3), RH142 (28), TB1 (4), and RP1 (23) (Fig. 1C).

Explant cocultivation reactivation assays. Following ocular infections with FS1001K and KOS, latent infections were established in the TG of mice. In Fig. 5, data from three independent explant cocultivation reactivation assays are summarized. Each experiment involved eyes and TG that were individually incubated for at least 28 days postexplantation from five latently infected BALB/c mice per virus. FS1001K reactivated from 20 of 30 TG (67%), whereas the WT parental KOS virus reactivated from 24 to 30 (80%). Reactivation of FS1001K was slightly delayed (half-life [$t_{1/2}$], 11 to 12 days) compared with that of KOS ($t_{1/2}$, 8 to 9 days [Fig. 5]). No reactivation was observed from eyes explanted from mice latently infected with either KOS or FS1001K during a 48-day observation period.

TABLE 2. *Xba*I, *Bgl*II, and *Bgl*II-*Xba*I restriction endonuclease DNA profiles of HSV-1 strains 17^+ and KOS and the variant FS1001K

Restriction endonuclease	Molecular weight[a]		
	17^+	KOS	FS1001K[b]
*Xba*I[b]	38.85 (a)	34.40 (a)	
	24.25 (b)	23.30 (b)	21.13 (b′)
	22.30 (c)	21.10 (c)	21.10 (c)
	18.59 (d)	18.20 (d)	20.48 (a′)
	18.66 (e)	18.00 (e)	18.00 (e)
	16.19 (f)	15.20 (f)	15.20 (f)
			14.20 (d′)
	06.98 (g)	07.10 (g)	
			03.87 (g′)
			03.22 (d′)
			02.45 (g′)
a=d+[S]			
b=g+[S]			
*Bgl*II[c]	23.65 (a)	23.80 (a)	23.02 (a′)
	20.89 (b)	20.50 (b)	19.72 (b′)
	18.58 (c)	19.10 (c)	18.32 (c′)
	17.00 (d)	16.80 (d)	16.80 (d)
	15.82 (e)	15.80 (e)	15.02 (e′)
	12.34 (f)	13.00 (f)	12.22 (f′)
	11.42 (g)	11.20 (g)	11.20 (g)
	11.31 (h)	10.80 (h)	10.80 (h)
	10.26 (i)	10.20 (i)	10.20 (i)
	09.58 (j)	09.70 (j)	08.92 (j′)
	06.94 (h)	06.80 (i)	06.80 (h)
	06.24 (l)	06.10 (l)	06.10 (l)
	04.21 (m)	04.00 (m)	04.00 (m)
	03.76 (n)	03.70 (n)	03.70 (n)
	03.48 (o)	03.40 (o)	03.40 (o)
	03.04 (p)	03.00 (p)	03.00 (p)
	00.28 (ln)	—[d] (ln)	— (ln)
	00.15 (ln)	— (ln)	— (ln)
a=f+h			
b=j+h			
c=f+l			
e=j+l			

Continued

TABLE 2—*Continued*

Restriction endonuclease	Molecular weight (10^6)[a]		
	17^+	KOS	FS1001K[b]
*Bgl*II-*Xba*I	23.65 (a)	23.80 (a)	
	18.58 (c)	19.10 (c)	
	18.29 (b)	17.90 (b′)	
			14.62 (b″)
			14.30 (a′)
	13.22 (e′)	13.20 (e′)	
	13.21 (d′)	13.10 (d′)	13.10 (d′)
	12.34 (f)	13.00 (f)	
	11.31 (h)	10.80 (h)	10.80 (h)
	10.26 (i)	10.20 (i)	10.20 (i)
			09.92 (e″)
			09.60 (c′)
			08.72 (f′)
	06.98 (j′)	07.10 (j′)	
	06.94 (k)	06.80 (k)	06.80 (k)
	06.24 (l)	06.10 (l)	06.10 (l)
	05.96 (g′)	05.90 (g′)	05.90 (g′)
	05.46 (g′)	05.30 (g′)	05.30 (g′)
			03.82 (j″)
	03.79 (d′)	03.70 (d′)	03.70 (d′)
	03.76 (n)	03.70 (n)	03.70 (n)
			03.50 (f′)
	03.48 (o)	03.40 (o)	03.40 (o)
	03.04 (p)	03.00 (p)	03.00 (p)
	02.60 (j′)	02.60 (j′)	02.60 (j′)
			02.50 (j″)
	02.15 (m′)	02.10 (m′)	02.10 (m′)
	02.06 (m′)	01.90 (m′)	01.90 (m′)

[a] Letters in parentheses refer to band designations of the indicated profiles. The molecular weights in the strain 17^+ column are based on HSV-1 DNA sequence information (39).

[b] Data in the KOS column are from Skare and Summers (55). The presence of an additional *Xba*I site and a 0.78×10^6 molecular weight deletion generated the a′, b′, d′, and g′ bands in the *Xba*I profile of the variant FS1001K (see Fig. 3a and Fig. 4, lane 2).

[c] Data in the KOS column are based on the restriction endonuclease mapping data of HSV-1 strain KOS (26, 44). Because of the 0.78×10^6 molecular weight deletion in the R_L, the *Bgl*II fragments j and f are reduced by 0.78×10^6 and, consequently, the joint fragments a, b, c, and e are also reduced in the FS1001K profile.

[d] —, no data.

When the reactivated viruses from these experiments were analyzed with *Bam*HI, *Xba*I, and *Bgl*II-*Xba*I digestions of their ^{32}P-labelled DNAs, their genomes were found to be identical to those of input viruses, which suggests that the reactivation behavior of FS1001K was not due to some other alteration or contamination with the WT virus (data not shown). The slightly reduced reactivation frequency of FS1001K compared with that of the parental KOS virus was consistent in all three experiments, indicating that the 1,186-bp deletion in FS1001K has a minimal effect on explant cocultivation reactivation. In contrast, explant reactivation of mutants that have deletions in the LAT promoter region is significantly slower or less efficient than that of the wild-type virus (32, 60).

LAT and RL2 (ICP0) expression in tissue culture and LAT expression in latently infected mouse TG. The deletion in FS1001K was precisely generated in such a way that the RL2 (ICP0) gene and its regulatory sequences would not be affected. Therefore, while it was expected that the variant (FS1001K) would not produce the 2.0-kb LAT, it should produce an intact RL2 transcript. Therefore, RNAs extracted from BHK21/C13 cells infected with HSV-1 strains 17^+ and KOS and the variant FS1001K were Northern blotted and hybridized to a nick translated *Pst*I-*Mlu*I subfragment of the HSV-1 (F) *Bam*HI b DNA probe (Fig. 1B, 2B, and 6A) (59) or a nick translated *Pst*I-*Kpn*I fragment excised from plasmid pMF201 (Fig. 2B; data not shown). It can be seen in Fig. 6A that the *Pst*I-*Mlu*I DNA probe hybridized with RL2 mRNA in BHK21/C13 cells infected with two independent isolates of FS1001K (lanes 1 and 3) as strongly as with the parental WT strains KOS (lane 2) and 17^+ (lane 5) mRNAs. Identical results were obtained using the *Pst*I-*Kpn*I DNA probe (data not shown). This confirms that the RL2 gene is expressed in the HSV-1 LAT deletion variant FS1001K.

During a productive HSV-1 infection in tissue culture or in mice, only the 2.0-kb LAT is detected (56, 58). LAT expression is relatively limited in tissue culture cells compared with that of latently infected ganglia (56, 64, 71). In HSV-1-infected tissue culture cells, the 2.0-kb LAT is expressed as a late gene (58). Recently, it has also been shown that a 2.0-kb LAT-related transcript is detectable in tissue culture cells in the absence of the putative TATA box of the LAT promoter, which is possibly expressed from a cryptic promoter located near the 5′ end of the 2.0-kb LAT (25, 46). On the other hand, during latent HSV-1 infection in mice, the 2.0-, 1.5-, and 1.45-kb LATs are

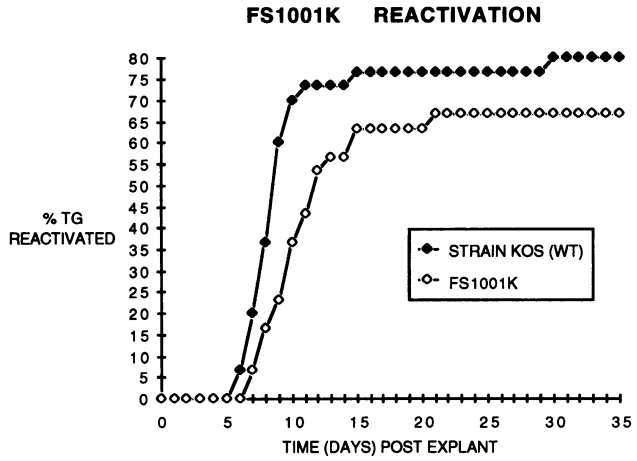

FIG. 5. Reactivation of HSV-1 strain KOS and the variant FS1001-K from latently infected BALB/c mouse TG following explant cocultivation. The assay was carried out on BHK21/C13 cell monolayers. The cell monolayers were observed daily for CPE. The ganglia were transferred onto fresh cell monolayers every 3 to 4 days and were monitored for 35 days. The data are compiled from three independent experiments.

all detectable and the 2.0-kb LAT is present at much higher levels than those during acute infection (56–58). To investigate whether the variant FS1001K produces the 2.0-kb LAT or the 2.0-kb LAT-related transcript in tissue culture and the 2.0-, 1.5-, and 1.45-kb LATs during the latent phase of infection in mice, RNAs from infected tissue culture cells and latently infected TG were analyzed by Northern blots using *Pst*I-*Mlu*I (Fig. 6) and *Pst*I-*Kpn*I (data not shown) DNA probes. No LAT transcripts were detected in productively infected tissue culture cells (Fig. 6A, lanes 1 and 3) or latently infected TG (Fig. 6B, lane 3) following infection with FS1001K. Identical results were obtained when RNAs extracted from FS1001K-infected BHK21/C13 cells harvested at 8 h (Fig. 6) and at 15 h (data not shown) postinfection were analyzed by Northern blots. In addition, as shown in Fig. 6C, the autoradiograph was exposed seven times longer than that shown in Fig. 6B to emphasize that the 2.0-, 1.5-, and 1.45-kb LATs are not detectable during latent FS1001K infection. Even when the autoradiograph was exposed for 19 days (~50 times), no LATs were detectable (data not shown). These results confirm that the deletion in FS1001K abolishes LAT expression in vitro and in vivo. However, it should be noted that the 2.0-kb LAT in strain KOS (Fig. 6B and C, lane 4) migrated slightly more slowly than that of strain 17^+ (Fig. 6B and C, lane 1) and that the 1.45- to 1.5-kb LAT transcripts are less abundant (~5 to 10%) and larger in strain KOS than those in strain 17^+ (64, 65). It should also be noted that no truncated or aberrant forms of the 2.0-kb LAT were observed, as described by Block et al. (3, 4).

DISCUSSION

FS1001K is the first HSV-1 LAT deletion variant in which the 2.0-kb LAT is precisely deleted from its 5′ end and in which both the large (ORF1) and small (ORF2) ORFs located entirely within the 2.0-kb LAT (59) are disrupted. Most other LAT variants have deletions and/or insertions in the putative LAT promoter region or the sequences upstream from the 5′ end of the 2.0-kb LAT (3, 28, 29, 32, 53, 54, 60, 63), along with

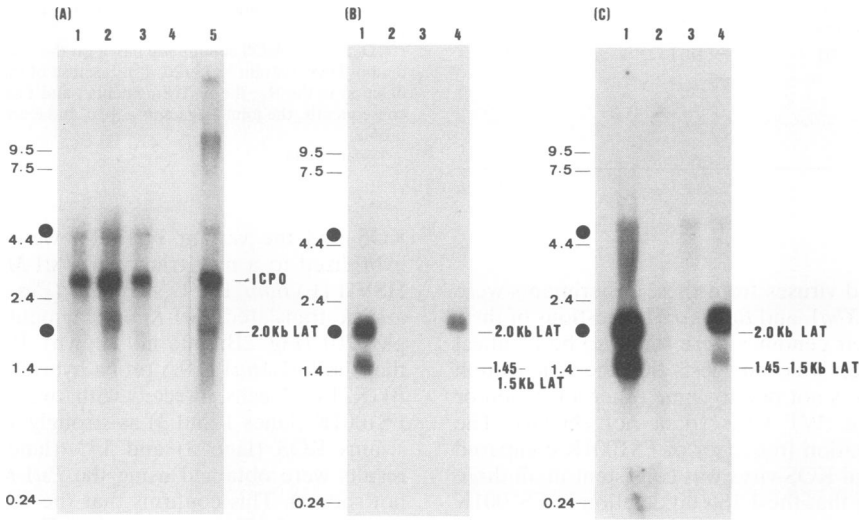

FIG. 6. Northern blot analysis of HSV-1 LATs and RL2 (ICP0) RNAs. (A) Lanes 1 and 3, 5 μg of RNA from different isolates of HSV-1 variant FS1001K-infected BHK21/C13 cells [MOI of 4) at 8 h postinfecction; lane 2, 5 μg of RNA from HSV-1 strain KOS-infected BHK21/C13 cells (MOI of 4) at 8 h postinfection; lane 4, 5 μg of RNA from mock-infected BHK21/C13 cells; lane 5, 5 μg of RNA from HSV-1 strain 17^+-infected BHK21/C13 cells (MOI of 4) at 8 h postinfection; (B) 5 μg of RNA from the TG of mice latently infected with HSV-1 strain 17^+ (lane 1), variant FS1001K (lane 3), and strain KOS (lane 4); lane 2, 5 μg of uninfected mouse brain RNA; (C) same as for panel B (9-h exposure), but with exposure for 62 h to show that the LATs are not detectable during FS1001K latency. The HSV-1 strain F *Pst*I-*Mlu*I subfragment of *Bam*HI b (as shown above) and the HSV-1 strain 17^+ *Pst*I-*Kpn*I fragment excised from plasmid pMF201 (see Fig. 2; data not shown) were used as ICP0-LAT dual probes (Fig. 1) (59). The autoradiograph was made with XAR-5 film (Kodak). The positions of RNA markers are labelled in kilobases on the left-hand side of each panel. The positions of the 2.0-kb and 1.45- to 1.50-kb LATs and RL2 (ICP0) are labelled on the right-hand side. The marked positions of the 2.0-kb and 1.45- to 1.50-kb LATs represent those of HSV-1 strain 17^+ (panel A, lane 5 and panels B and C, lane 1). These LTs are larger in HSV-1 strain KOS (panel A, lane 2 and panels B and C, lane 4) than those in strain 17^+. The 28S and 18S rRNAs are indicated by filled circles.

some of the 2.0-kb LAT sequences. The DNA sequences just upstream of the 5′ end of the 2.0-kb LAT may contain a second promoter which is functional during virus replication (25, 46). Latency studies with these variants have suggested that while the LATs are not essential for virus replication (in vitro and in vivo) or establishment or maintenance of latency, the LATs may facilitate reactivation in both explant cocultivation assays (in vitro) and animal models (in vivo). However, three HSV-1 variants, RH142 (28), TB1 (4), and RP1 (23), with intact LAT promoters and ORF2 sequences (Fig. 1) reactivate normally. In HSV-1 strain KOS variant RH142, a 373-bp (nt 119,597 to 119,970) DNA fragment was replaced by the *LacZ* coding sequences, thus removing the splice donor site and a portion of the intron within the 2.0-kb LAT (59). TB1 was generated in an HSV-1 strain HFEM background, which contain a 4.1-kb deletion within the *Bam*HI b fragment and only one complete copy of LATs. A 168-bp *Hpa*I-*Hpa*I fragment (nt 5,902 to 6,070, which correspond to nt 120,300 to 120,468 in the IR_L) was replaced by a 440-bp *Hpa*I fragment of a lambda bacteriophage DNA and, in consequence, the ORF1 (nt 120,419 to 121,240) within the 2.0-kb LAT was disrupted (4). The HSV-1 strain 17^+ variant RP1 was constructed by inserting an 8-bp *Cla*I linker within the *Hpa*I (nt 120,468) restriction endonuclease site, therefore introducing a frameshift mutation near the 5′ end of ORF1 (23). All three virus variants (RH142, TB1, and RP1) reactivated efficiently, from either the TG of mice (RH142 and TB1) in cocultivation assays (in vitro) or from rabbits (RP1) in an induced and/or spontaneous in vivo animal model system. Thus, disruption of the intron or ORF1 within the 2.0-kb LAT does not affect the HSV-1 reactivation process. However, none of the reported variants has a precise deletion starting from the 5′ end of the 2.0-kb LAT or a deletion and/or insertion within ORF2 of the 2.0-kb LAT. Therefore, a variant (FS1001K) was generated to delete as much of the 2.0-kb LAT as possible without affecting the RL2 gene. The FS1001K reactivation data (Fig. 5) suggest that the first 1,186 bp of the 2.0-kb LAT, which include its putative ORFs, are not required for efficient explant reactivation. Although the reactivation profile of FS1001K from the latently infected TG of mice was found to be slightly less than that of the parental WT virus (Fig. 5), the difference was slight compared with the impaired reactivation of viruses with large deletions that encompass the LAT promoter (32, 60).

The reactivation behavior of LAT promoter variants is also controversial. For instance, Devi-Rao et al. (16) have recently shown that a LAT promoter deletion variant (KOS/29) in a strain KOS (M) background reactivated with WT kinetics in a murine footpad model, whereas an identical variant (17ΔPst) in a strain 17^+ background reactivated with significant but slight delay and with reduced frequency compared with the parental WT virus. Similar results were also obtained with the murine eye model (16) and the epinephrine-induced rabbit eye model (5) using 17^+ variant 17ΔPst; however, the behavior of the KOS (M) variant KOS/29 was not tested in the epinephrine-induced rabbit eye model. Moreover, Sawtell and Thompson (53), using the same virus (KOS/29) in a hyperthermia-induced murine model, have demonstrated that the virus reactivates like the WT from spinal ganglia but with reduced frequency from TG, suggesting the importance of anatomical location of the neuronal tissues in HSV reactivation. In addition, their studies indicate that LATs may also be involved during the establishment phase of latency. On the other hand, the explant reactivation profile of the variant KOS/29 has also been shown to be similar to that of the WT in a murine eye model (15). Therefore, it appears that the behavior of mutations within the LAT promoter region varies from strain to strain and from model to model, whereas that of the 2.0-kb LAT does not (3, 4, 23, 27–29, 32, 60, 63).

Mutations within the LATs that do not affect the putative LAT promoter region destabilize the LATs. For example, LATs are not detectable during HSV-1 variant RH142 (28) latency or virus replication in vitro. Similarly, no LATs are detected during RP1 (23) or TB1 (4) latency. In contrast, novel transcripts of 0.7 to 0.8 kb and 1.1 kb are detected in TB1- and 17N/H-infected tissue culture cells (3, 4). Therefore, it was important to investigate whether FS1001K produces any truncated form(s) of the 2.0-kb LAT. However, neither the 2.0-, 1.5-, and 1.45-kb LATs nor any other LAT could be detected in tissue culture cells or infected mouse TG (Fig. 6), even after longer exposure (~19 days). The 2.0-kb ORF1 and ORF2 are intact in RH142, whereas ORF2 is intact in TB1, 17N/H, and RP1. Therefore, it is possible that the aberrant transcirpts observed by Block et al. (3, 4) represent these ORFs along with the remaining 3′ end sequences of the 2.0-kb LAT.

The deletion and insertion in FS1001K abolish the splice donor signal at the 5′ end of the 2.0-kb LAT, since the consensus splice donor signal (A/C**AG**:**GT**A/G**AGT**) was changed from TTTCCAG:GTAGGTT to TTTCCAG:TCTA GAT (the nucleotides which differ from those of the consensus sequence are underlined [Table 1]). If the 2.0-kb LAT is an intron (22), it would not be expected to be spliced out in FS1001K during RNA processing and, consequently, no 6-kb LAT (m-LAT [8 − 2 kb = 6 kb]) would be made. In addition, the 1.45- to 1.5-kb LATs cannot be made because the intron (59) within the 2.0-kb LAT was completely deleted in FS1001K. In contrast, if the 2.0-kb LAT is a stable exon and its 5′ end actually contains a splice acceptor signal [consensus sequence, $(T/C)_{11}$NC/T**AG**:NNN; HSV-1 LAT, ACGCCGCG TTTCC**AG**:GTAGGT; FS1001K LAT, ACGCCGCGTTTC C**AG**:TCTAGA], a 0.77-kb truncated form of the stable LAT (1955 − 1186 = 769 bp) could be made by the variant FS1001K but might be unstable. In addition, the expected hypothetical m-LAT in FS1001K would be approximately 6.8 kb. However, no LATs were detected in vitro or in vivo with FS1001K (Fig. 6), suggesting that the possible LATs made by FS1001K were unstable or that the virus did not make any LATs. Since the LAT promoter is unaffected in FS1001K, it is more likely that any LATs that are synthesized are unstable. In both cases, the LATs are not essential for explant reactivation.

Since both TB1 (4) and RP1 (23) reactivated efficiently, it was considered that the LAT ORF2 may be functional in the reactivation process and that this ORF might also encode a gene product. In addition, Doerig et al. (18) have demonstrated a latency-associated antigen in cultured neurons recognized with antisera raised against a chimeric protein containing the carboxy-terminal part of the LAT ORF1 (several groups of researchers call this large ORF ORF2 [18, 23, 64–67]). Furthermore, this anti-LAT2 antiserum also recognized an 80-kDa protein and a 45-kDa protein in whole-cell extracts from an in vitro model of latently infected neurons. Therefore, one intention for generating the variant FS1001K included the investigation of a possible LAT gene product(s). We have indeed carried out some preliminary experiments to identify HSV-1 2.0-kb LAT ORF2 gene product(s) in infected tissue culture cells and in latently infected tissues, and attempts were also made to express such proteins in bacterial expression systems; however, these experiments are still inconclusive (21).

The results obtained with FS1001K and described herein indicate that neither of the ORFs within the 2.0-kb and also contained within the 1.45- to 1.5-kb LATs are required for the establishment of latency or reactivation from latency. If the LAT-specific sequences do encode any protein(s) involved in

reactivation, they are located outside the boundaries of the 2.0-kb LAT. Alternatively, the LAT gene might act through a functional RNA molecule. In either case, the region of the LAT gene involved in reactivation maps outside the region of the FS1001K deletion.

ACKNOWLEDGMENTS

We are grateful to Nigel W. Fraser for critical reading of the manuscript, advice, and useful discussions.

This work was supported by program project grant A1-23968 from the National Institutes of Health.

REFERENCES

1. **Baines, J. D., and B. Roizman.** 1991. The open reading frames UL3, UL4, UL10 and UL16 are dispensable for the growth of herpes simplex virus 1 in cell culture. J. Virol. **65**:938–944.
2. **Birnboim, H. C., and J. Doly.** 1979. A rapid alkaline extraction procedure for screening recombinant plasmid DNA. Nucleic Acids Res. **7**:1513–1523.
3. **Block, T. M., S. Deshmane, J. Masonis, J. Maggioncalda, T. Valyi-Nagi, and N. W. Fraser.** 1993. An HSV LAT null mutant reactivates slowly from latent infection and makes small plaques on CV-1 monolayers. Virology **192**:618–630.
4. **Block, T. M., J. G. Spivack, I. Steiner, S. Deshmane, R. P. Lirette, M. McIntosh, and N. W. Fraser.** 1990. A herpes simplex virus type 1 latency-associated transcript mutant reactivates with normal kinetics from latent infection. J. Virol. **64**:3417–3426.
5. **Bloom, D. C., G. B. Devi-Rao, J. M. Hill, J. G. Stevens, and E. K. Wagner.** 1994. Molecular analysis of herpes simplex virus type 1 during epinephrine-induced reactivation of latently infected rabbits in vivo. J. Virol. **68**:1283–1292.
6. **Brown, S. M., J. Harland, and J. H. Subak-Sharpe.** 1984. Isolation of restriction endonuclease site deletion mutants of herpes simplex virus. J. Gen. Virol. **65**:1053–1068.
7. **Brown, S. M., D. A. Ritchie, and J. H. Subak-Sharpe.** 1973. Genetic studies with herpes simplex virus type 1. The isolation of temperature-sensitive mutants, their arrangement into complementation groups and recombination analysis leading to a linkage map. J. Gen. Virol. **18**:329–346.
8. **Chou, J., E. R. Kern, R. J. Whitley, and B. Roizman.** 1990. Mapping of herpes simplex virus-1 neurovirulence to γ1 34.5, a gene nonessential for growth in culture. Science **250**:1262–1265.
9. **Copertino, D. W., and R. B. Hallick.** 1991. Group II twintron: an intron within an intron in a chloroplast cytochrome b-559 gene. EMBO J. **10**:433–442.
10. **Davison, A. J.** 1981. Detailed structural aspects of the herpes simplex virus genome. Ph.D. thesis. University of Glasgow, Glasgow, Scotland.
11. **Davison, A. J., and N. M. Wilkie.** 1981. Nucleotide sequences of the joint between the L and S segments of herpes simplex virus types 1 and 2. J. Gen. Virol. **55**:315–331.
12. **Deatly, A. M., J. G. Spivack, E. Lavi, and N. W. Fraser.** 1987. RNA from an immediate early region of the HSV-1 genome is present in the trigeminal ganglia of latently infected mice. Proc. Natl. Acad. Sci. USA **84**:3204–3208.
13. **Deatly, A. M., J. G. Spivack, E. Lavi, D. R. O'Boyle II, and N. W. Fraser.** 1988. Latent herpes simplex virus type 1 transcripts in peripheral and central nervous system tissues of mice map to similar regions of the viral genome. J. Virol. **62**:749–756.
14. **Deshmane, S. L., and N. W. Fraser.** 1989. During latency, herpes simplex virus type 1 DNA is associated with nucleosomes in a chromatin structure. J. Virol. **63**:943–947.
15. **Deshmane, S. L., M. Nicosia, T. Valyi-Nagy, L. T. Feldman, A. Dillner, and N. W. Fraser.** 1993. An HSV-1 mutant lacking the LAT TATA element reactivates normally in explant cocultivation. Virology **196**:868–872.
16. **Devi-Rao, G. B., D. C. Bloom, J. G. Stevens, and E. K. Wagner.** 1994. herpes simplex virus type 1 DNA replication and gene expression during explant-induced reactivation of latently infected murine sensory ganglia. J. Virol. **68**:1271–1282.
17. **Dobson, A. T., F. Sedarati, G. Devi-Rao, W. M. Flanagan, M. J. Farrell, J. G. Stevens, E. K. Wagner, and L. T. Feldman.** 1989. Identification of the latency-associated transcript promoter by expression of rabbit beta-globin mRNA in mouse sensory nerve ganglia latently infected with a recombinant herpes simplex virus. J. Virol. **63**:3844–3851.
18. **Doerig, C., L. I. Pizer, and C. L. Wilcox.** 1991. An antigen encoded by the latency-associated transcript in neuronal cell culture latently infected with herpes simplex virus type 1. J. Virol. **65**:2724–2727.
19. **Efstathiou, S., A. C. Minson, H. J. Field, J. R. Anderson, and P. Wildly.** 1986. Detection of herpes simplex virus-specific DNA sequences in latently infected mice and in humans. J. Virol. **57**:446–455.
20. **Fareed, M. U.** 1992. Isolation of herpes simplex virus type 1 variants devoid of *Hind III* RE sites and their use in intrastrain recombination studies. Ph.D. thesis. University of Glasgow, Glasgow, Scotland.
21. **Fareed, M. U., Z. Wroblewska, J. Otto, and J. G. Spivack.** Unpublished data.
22. **Farrell, M. J., A. T. Dobson, and L. T. Feldman.** 1991. Herpes simplex virus latency-associated transcript is a stable intron. Proc. Natl. Acad. Sci. USA **88**:790–794.
23. **Farrell, M. J., J. M. Hill, T. P. Margolis, J. G. Stevens, E. K. Wagner, and L. T. Feldman.** 1993. The herpes simplex virus type 1 reactivation function lies outside the latency-associated transcript open reading frame ORF-2. J. Virol. **67**:3653–3655.
24. **Fraser, N. W., T. M. Block, and J. G. Spivack.** 1992. The latency-associated transcripts of herpes simplex virus: RNA in search of function. Virology **191**:1–8.
25. **Goins, W. F., L. R. Sternberg, K. D. Croen, P. R. Krause, R. L. Hendricks, D. J. Fink, S. E. Straus, M. Levine, and J. C. Glorioso.** 1994. A novel latency-active promoter is contained within the herpes simplex virus type 1 U_L flanking repeats. J. Virol. **68**:2239–2252.
26. **Goldin, A. L., R. M. Sandri-Goldin, M. Levine, and J. C. Glorioso.** 1981. Cloning of herpes simplex virus type 1 sequences representing the whole genome. J. Virol. **38**:50–58.
27. **Hill, J. M., F. Sederati, R. T. Javier, E. K. Wagner, and J. G. Stevens.** 1990. herpes simplex virus latent phase transcription facilitates in vivo reactivation. Virology **174**:117–125.
28. **Ho, D. Y., and E. S. Mocarski.** 1989. Herpes simplex virus latent RNA (LAT) is not required for latent infection in the mouse. Proc. Natl. Acad. Sci. USA **86**:7596–7600.
29. **Javier, R. T., J. G. Stevens, V. B. Dissette, and E. K. Wagner.** 1988. A herpes simplex virus transcript abundant in latently infected neurons is dispensable for establishment of the latent state. Virology **166**:254–257.
30. **Kunkel, T. A.** 1985. Rapid and efficient site-specific mutagenesis without phenotypic selection. Proc. Natl. Acad. Sci. USA **82**:488–492.
31. **Kunkel, T. A., J. D. Roberts, and R. A. Zakour.** 1987. Rapid and efficient site-specific mutagensis without phenotypic selection. Methods Enzymol. **154**:367–382.
32. **Leib, D. A., C. L. Bogard, M. Kosz-Vnenchak, K. A. Hicks, D. M. Coen, D. M. Knipe, and P. A. Schaffer.** 1989. A deletion mutant of the latency-associated transcript of herpes simplex virus type 1 reactivates from the latent state with reduced frequency. J. Virol. **63**:2893–2900.
33. **Lonsdale, D. M.** 1979. A rapid technique for distinguishing herpes simplex virus type 1 from type 2 by restriction enzyme technology. Lancet **i**:849–852.
34. **Lonsdale, D. M., S. M. Brown, J. Lang, J. H. Subak-Sharpe, H. Koprowski, and K. G. Warren.** 1980. Variations in herpes simplex virus isolated from human ganglia and a study of clonal variations in HSV-1. Ann. N. Y. Acad. Sci. **354**:291–308.
35. **MacLean, A. R., and S. M. Brown.** 1987. A herpes simplex virus type 1 variant which fails to synthesize immediate early polypeptide VmwIE63. J. Gen. Virol. **68**:1339–1350.
36. **MacLean, A. R., M. U. Fareed, L. Robertson, J. Harland, and S. M. Brown.** 1991. Herpes simplex virus type 1 deletion variants 1714 and 1716 pinpoint neurovirulence-related sequences in Glasgow strain 17^+ between immediate early gene 1 and the 'a' sequence. J. Gen. Virol. **72**:631–639.
37. **MacPherson, I., and M. G. Stoker.** 1962. Polyoma transformation

of hamster cell clones—an investigation of genetic factors affecting cell competence. Virology **16:**147–151.

38. **Margolis, T. P., D. C. Bloom, A. T. Dobson, L. T. Feldman, and J. G. Stevens.** 1993. Decreased reporter gene expression during latent infection with HSV LAT promoter constructs. Virology **197:** 585–592.
39. **McGeoch, D. J., M. A. Dalrymple, A. J. Davison, A. Dolan, M. C. Frame, D. McNab, L. J. Perry, J. E. Scott, and P. Taylor.** 1988. The complete DNA sequence of the long unique region in the genome of herpes simplex virus type 1. J. Gen. Virol. **69:**1531–1574.
40. **Mead, D. A., E. Szczesna-Skorupa, and B. Kemper.** 1986. Single stranded 'blue' T7 promoter plasmids: a versatile tandem promoter system for cloning and protein engineering. Protein Eng. **1:**67–74.
41. **Mellerick, D. M., and N. W. Fraser.** 1987. Physical state of the latent herpes simplex virus genome in a mouse model system: evidence suggesting an episomal state. Virology **158:**265–275.
42. **Mitchell, W. J., R. P. Lirette, and N. W. Fraser.** 1990. Mapping of low abundance latency-associated RNA in the trigeminal ganglia of mice latently infected with herpes simplex virus type 1. J. Gen. Virol. **71:**125–132.
43. **Mitchell, W. J., I. Steiner, S. M. Brown, A. R. MacLean, J. H. Subak-Sharpe, and N. W. Fraser.** 1990. A herpes simplex virus type 1 variant, deleted in the promoter region of the latency-associated transcripts, does not produce any detectable minor RNA species during latency in the mouse trigeminal ganglion. J. Gen. Virol. **71:**953–957.
44. **Morse, L. S., T. G. Buchman, B. Roizman, and P. A. Schaffer.** 1977. Anatomy of herpes simplex virus DNA. IX. Apparent exclusion of some parental DNA arrangements in the generation of intertypic (HSV-1 × HSV-2) recombinants. J. Virol. **24:**231–248.
45. **Mullaney, J., H. W. M. Moss, and D. J. McGeoch.** 1989. Gene UL2 of herpes simplex virus type 1 encodes a uracil-DNA glycosylase. J. Gen. Virol. **70:**449–454.
46. **Nicosia, M., S. L. Deshmane, J. M. Zabolotny, T. Valyi-Nagy, and N. W. Fraser.** 1993. Herpes simplex virus type 1 latency-associated transcript (LAT) promoter deletion mutants can express a 2-kilobase transcript mapping to the LAT region. J. Virol. **67:**7276–7283.
47. **Post, L. E., and B. Roizman.** 1981. A generalized technique for deletion of specific genes in large genomes: α gene 22 of herpes simplex virus 1 is not essential for growth. Cell **25:**227–232.
48. **Puga, A., J. D. Rosenthal, H. Openshaw, and A. L. Notkins.** 1978. Herpes simplex virus DNA and mRNA sequences in acutely and chronically infected trigeminal ganglia of mice. Virology **89:**102–111.
49. **Rock, D. L., and N. W. Fraser.** 1983. Detection of HSV-1 genome in central nervous system of latently infected mice. Nature (London) **302:**523–525.
50. **Rock, D. L., A. B. Nesburn, H. Ghiasi, J. Ong, T. L. Lewis, J. R. Lokensgard, and S. L. Wechsler.** 1987. Detection of latency related viral RNAs in trigeminal ganglia of rabbits latently infected with herpes simplex virus type 1. J. Virol. **61:**3820–3826.
51. **Sambrook, J., E. F. Fritsch, and T. Maniatis.** 1989. Molecular cloning: a laboratory manual, 2nd ed. Cold Spring Harbor Laboratory Press, Cold Spring Harbor, N.Y.
52. **Sandri-Goldin, R. M., M. Levine, and J. C. Glorioso.** 1981. Method for induction of mutations in physically defined regions of the herpes simplex virus genome. J. Virol. **38:**41–49.
53. **Sawtell, N. M., and R. L. Thompson.** 1992. Herpes simplex virus type 1 latency-associated transcription unit promotes anatomical site-dependent establishment and reactivation from latency. J. Virol. **62:**2157–2169.
54. **Sedarati, F., K. M. Izumi, E. K. Wagner, and J. G. Stevens.** 1989. Herpes simplex virus type 1 latency-associated transcription plays no role in establishment or maintenance of a latent infection in murine sensory neurons. J. Virol. **63:**4455–4458.
55. **Skare, J., and W. C. Summers.** 1977. Structure and function of herpesvirus genomes. II. *Eco*RI, *Xba*I, and *Hin*dIII endonuclease cleavage sites on herpes simplex virus type 1 DNA. Virology **76:** 581–595.
56. **Spivack, J. G., and N. W. Fraser.** 1987. Detection of herpes simplex virus type 1 transcripts during latent infection in mice. J. Virol. **61:**3841–3847.
57. **Spivack, J. G., and N. W. Fraser.** 1988. Expression of herpes simplex virus type 1 latency-associated transcripts in the trigeminal ganglia of mice during acute infection and reactivation of latent infection. J. Virol. **62:**1479–1485.
58. **Spivack, J. G., and N. W. Fraser.** 1988. Expression of herpes simplex virus type 1 (HSV-1) latency-associated transcripts and transcripts affected by the deletion in avirulent mutant HFEM: evidence for a new class of HSV-1 genes. J. Virol. **62:**3281–3287.
59. **Spivack, J. G., G. M. Woods, and N. W. Fraser.** 1991. Identification of a novel latency-specific splice donor signal within the herpes simplex virus type 1 2.0-kilobase latency-associated transcript (LAT): translation inhibition of LAT open reading frame by the intron within the 2.0-kilobase LAT. J. Virol. **65:**6800–6810.
60. **Steiner, I., J. G. Spivack, R. P. Lirrette, S. M. Brown, A. R. MacLean, J. H. Subak-Sharpe, and N. W. Fraser.** 1989. herpes simplex virus latency-associated transcripts are evidently not essential for latent infection. EMBO J. **8:**505–511.
61. **Stevens, J. G., E. K. Wagner, G. B. Devi-Rao, M. L. Cook, and L. T. Feldman.** 1987. RNA complementary to a herpesvirus α gene mRNA is prominent in latently infected neurons. Science **235:** 1056–1059.
62. **Stow, N. D., and N. M. Wilkie.** 1976. An improved technique for obtaining enhanced infectivity with herpes simplex virus type 1 DNA. J. Gen. Virol. **33:**447–458.
63. **Trousdale, M. D., I. Steiner, J. G. Spivack, S. L. Deshmane, S. M. Brown, A. R. MacLean, J. H. Subak-Sharpe, and N. W. Fraser.** 1991. In vivo and in vitro reactivation impairment of a herpes simplex virus type 1 latency-associated transcript variant in a rabbit eye model. J. Virol. **65:**6989–6993.
64. **Wagner, E. K., G. Devi-Rao, L. T. Feldman, A. T. Dobson, Y.-F. Zhang, W. M. Flanagan, and J. G. Stevens.** 1988. Physical characterization of the herpes simplex virus latency-associated transcripts in neurons. J. Virol. **62:**1194–1202.
65. **Wagner, E. K., W. M. Flanagan, G. Devi-Rao, Y.-F. Zhang, J. M. Hill, K. P. Anderson, and J. G. Stevens.** 1988. The herpes simplex virus latency-associated transcript is spliced during the latent phase of infection. J. Virol. **62:**4577–4585.
66. **Wechsler, S. L., A. B. Nesburn, R. Watson, S. M. Slanina, and H. Ghiasi.** 1988. Fine mapping of the latency-related gene of herpes simplex virus type 1: alternate splicing produces distinct latency-related RNAs containing open reading frames. J. Virol. **62:**4051–4058.
67. **Wechsler, S. L., A. B. Nesburn, J. Zwaagstra, and H. Ghiasi.** 1989. Sequence of the latency-related gene of herpes simplex virus type 1. Virology **168:**168–172.
68. **Wilkie, N. M.** 1973. The synthesis and substructure of herpesvirus DNA: the distribution of alkali-labile single strand interruptions in HSV-1 DNA. J. Gen. Virol. **21:**453–467.
69. **Wilkie, N. M.** 1976. Physical maps for herpes simplex virus type 1 DNA for restriction endonucleases *Hind* III, *Hpa*-1 and *X. bad.* J. Virol. **20:**222–233.
70. **Wilkie, N. M., R. Cortini, and J. B. Clements.** 1977. Structural studies and physical maps for the herpes simplex virus genome. J. Antimicrob. Chemother. **3:**47–62.
71. **Zwaagstra, J., H. Ghiasi, A. B. Nesburn, and S. L. Wechsler.** 1989. In vitro promoter activity associated with the latency-associated transcript gene of herpes simplex virus type 1. J. Gen. Virol. **70:** 2163–2169.
72. **Zwaagstra, J., H. Ghiasi, S. M. Slanina, A. B. Nesburn, S. C. Wheatley, K. Lillycrop, J. Wood, D. S. Latchman, K. Patel, and S. L. Wechsler.** 1990. Activity of herpes simplex virus type 1 latency associated transcript (LAT) promoter in neuron-derived cells: evidence for neuron specificity and for a large LAT transcript. J. Virol. **64:**5019–5028.